

# Electric contact stability of anti-wear probes

Yasushi Tomizawa<sup>1,2,3a)</sup>, Yongfang Li<sup>1,2</sup>, Akihiro Koga<sup>1,2</sup>,  
Hiroshi Toshiyoshi<sup>3</sup>, Yasuhisa Ando<sup>1,4</sup>, Gen Hashiguchi<sup>1,5</sup>,  
and Hiroyuki Fujita<sup>1,6</sup>

<sup>1</sup> 3D-BEANS Center, BEANS Laboratory,

As-405, 4–6–1 Komaba, Meguro-ku, Tokyo 153–8505, Japan

<sup>2</sup> Corporate R&D Center, Toshiba Corporation

<sup>3</sup> Research Center for Advanced Science and Technology, the University of Tokyo

<sup>4</sup> Tokyo University of Agriculture and Technology

<sup>5</sup> Shizuoka University

<sup>6</sup> Institute of Industrial Science, the University of Tokyo

a) [yasushi.tomizawa@toshiba.co.jp](mailto:yasushi.tomizawa@toshiba.co.jp)

**Abstract:** For the practical realization of precise processes or devices utilizing scanning nanoprobe, not only improvement in the wear resistance of the probe tip but also a stable electric contact at the sliding probe electrode is required. To meet both these requirements, the authors developed an anti-wear probe having a supporting Si tip and a metal electrode, both of which slide on the substrate simultaneously. Probes with various electrode materials were evaluated to investigate the key factors of the material choice for maintaining good electric contact over a long sliding distance. The results show that the optimal management of material hardness, surface roughness, and probe contact force was important to realize an optimum performance from the probe.

**Keywords:** MEMS, electric contact, anti-wear probe, tribology

**Classification:** Micro- or nano-electromechanical systems

## References

- [1] K. Kakushima, T. Watanabe, K. Shimamoto, T. Couda, M. Ataka, H. Mimura, Y. Isono, G. Hashiguchi, Y. Mihara, and H. Fujita, “Atomic Force Microscope Cantilever Array for Parallel Lithography of Quantum Devices,” *Jpn. J. Appl. Phys.*, vol. 43, no. 6B, pp. 4041–4044, June 2004.
- [2] E. Eleftheriou, T. Antonakopoulos, G. K. Binnig, G. Cherubini, M. Despont, A. Dholakia, U. Durig, M. A. Lantz, H. Pozidis, H. E. Rothuizen, and P. Vettiger, “Millipede-A MEMS-Based Scanning-Probe Data-Storage System,” *IEEE Trans. Magn.*, vol. 39, no. 2, pp. 938–945, March 2003.
- [3] K. Tanaka, Y. Kurihara, T. Uda, Y. Daimon, N. Odagawa, R. Hirose, Y. Hiranaga, and Y. Cho, “Scanning Nonlinear Dielectric Microscopy Nano-Science and Technology for Next Generation High Density Ferroelectric Data Storage,” *Jpn. J. Appl. Phys.*, vol. 47, no. 5, pp. 3311–3325, May 2008.

- [4] Y. F. Li, Y. Tomizawa, A. Koga, G. Hashiguchi, M. Sugiyama, and H. Fujita, “A Trench-Type Anti-Wear Microprobe with Nano-Scale Electric Contacts for AFM LAO Lithography,” *Proc. IEEE Int. Conf. Micro Electro Mechanical Systems - MEMS2011*, Cancun, Mexico, pp. 1337–1340, Jan. 2011.
- [5] Y. Tomizawa, Y. Ando, and H. Fujita, “Electric Contact Characteristics at the Nanoscale Probe Tip,” *Transactions of the Japan Society of Mechanical Engineers C*, vol. 78, no. 786, pp. 267–278, Feb. 2012, In Japanese.
- [6] D. Tabor, *The Hardness of Metals*, Clarendon Press, Oxford, 1951.

## 1 Introduction

Precise processes or devices utilizing scanning nanoprobe, e.g., probe-based nanolithography [1] and probe-based data storage [2, 3], are state-of-the-art technologies that can handle tiny nanometer-sized patterns. To transfer these technologies from the research and development stage to practical implementation, several tribological requirements must be satisfied; first, a significant improvement in the wear resistance of the probe tip is required for a reliable and long-term operation of the system. Furthermore, to remove the unevenness of drawn patterns or recorded bits, the electric contact at the nanoscale sliding contact area must be stable.

To satisfy both of these requirements, the authors developed an anti-wear probe fabricated by micro electro-mechanical systems (MEMS) technology [4]. The probe consisted of a nondoped Si cantilever and a metal electrode (Fig. 1 (a)). There were two types of anti-wear probe, and in both the types, the surfaces of the Si support and the electrode made contact and slid simultaneously on the substrate. Despite the fact that the electric contact area of the electrode was as small as that of a conventional sharp probe tip, the physical contact area of the tip was larger than that of the conventional one, and the wear-progression speed therefore reduced. Using the anti-wear probe (type B), the authors performed an experiment involving the local anodic oxidation (LAO) lithography of Si wafers, and succeeded in drawing the line patterns with a uniform width both before and after a 20 mm slide [4].

However, to achieve stable drawing during the slide over a distance of more than several meters, a more detailed investigation of the electric and physical contact phenomena at the tip of the anti-wear probe is needed. It is important to understand the relation between the electric contact stability and the key properties of the materials that constitute the sliding system (the probe electrode, probe cantilever, and substrate). For this purpose, the authors performed the direct measurement of the electric current during the slide.

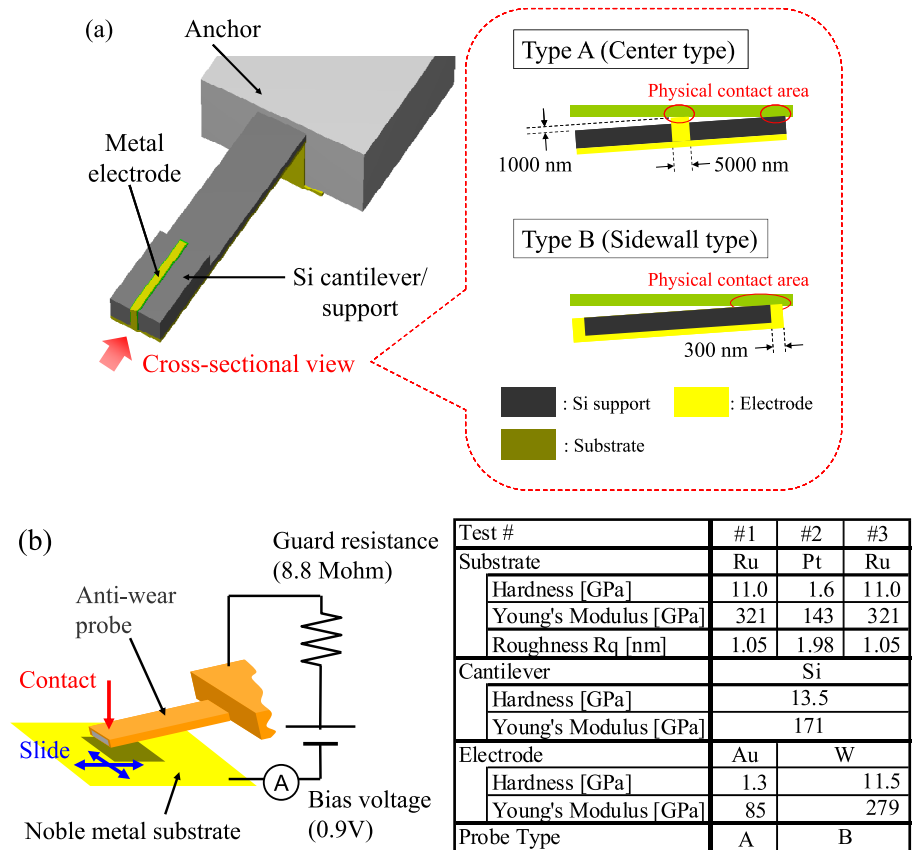


**Fig. 1.** (a) Schematic of the anti-wear probes, and (b) their sliding tests

## 2 Measurement

The sliding tests of the fabricated probes were performed using the contact mode of the atomic force microscopy (AFM) system which can apply a bias voltage to the substrate holder and measure the electric current flowing through the contact area at the probe tip electrode. The probe tip was pressed against the surface of the noble metal substrates (polished single crystal Pt and Ru) with a contact force of about  $1 \mu\text{N}$ , and it was scanned at  $20 \mu\text{m/s}$  on the substrate within a  $10 \mu\text{m} \times 10 \mu\text{m}$  observation area. The AFM images and current images (2D mapping of electric current distribution) were taken while scanning. The pitch between each scan line is about  $78 \text{ nm}$  (128 scan lines per image). The measurements were performed repeatedly until the cumulative sliding distance exceeded  $50 \text{ mm}$ .

Before the measurement, the substrates were cleaned using an organic solvent and baked at  $300^\circ\text{C}$  for  $1 \text{ h}$  in a vacuum to remove contaminants or water molecules stuck onto the substrate surface. The measurements were performed in vacuum atmosphere ( $10^{-4}$ – $10^{-3} \text{ Pa}$ ), at room temperature. The measurement range of electric current was  $0$ – $40 \text{ nA}$ .

We performed the tests using three different combinations of the electrode material and the substrate material. Details of the conditions for each test are shown in Fig. 1 (b). In tests #2 and #3, the observation area on the substrate was changed at about every  $10 \text{ mm}$  sliding distance, whereas test

#1 was performed entirely in the same observation area. The hardness and the Young's modulus of the materials were measured by nanoindentation. The surface roughness of the substrates was described in  $R_q$  (root mean squared) values, which was measured by tapping mode AFM. The length, width, and thickness of the Si cantilever beam of the probe are  $450\text{ }\mu\text{m}$ ,  $100\text{ }\mu\text{m}$ , and about  $5\text{ }\mu\text{m}$ , respectively. The dimensions of the electrodes are shown in Fig. 1 (a).

After the sliding tests, the tips of the probes used in the tests were observed by a field emission scanning electron microscope (FE-SEM) for a detailed investigation of the physical contact situation and the probe tip wear.

### 3 Results

The current images obtained during the sliding test at the first scan, the scan after the 25 mm slide, and the scan after the 50 mm slide are shown in Fig. 2 (a). The white area in the image shows electric currents greater than  $40\text{ nA}$ , which indicates that a good electric contact is observed between

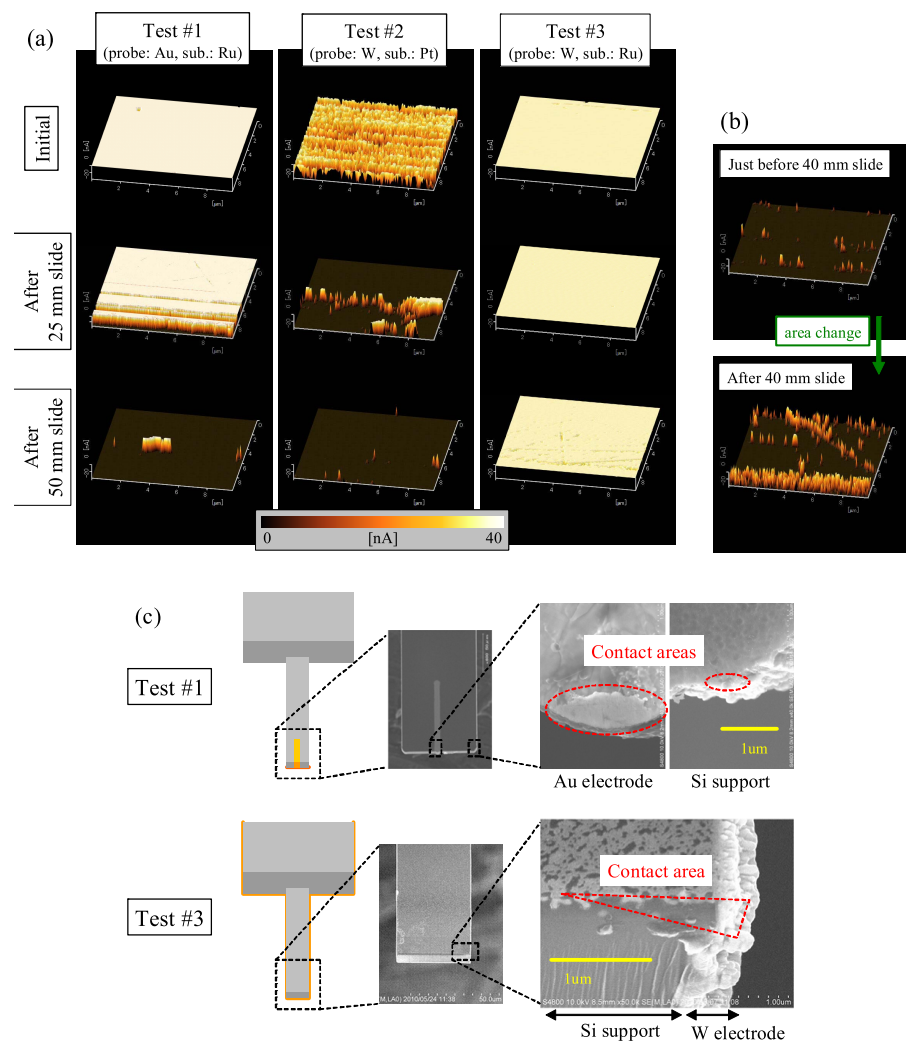


**Fig. 2.** Results of the sliding tests: (a) current images of all tests, (b) images before and after 40 mm slide in test #2, and (c) FE-SEM images

the probe electrode and the substrate, whereas the black area indicates no electric current flow.

In test #1, using the probe type A with an Au electrode, the overall current image was initially white, which indicates that an excellent electric contact between the Au electrode and the Ru substrate was maintained while the probe was sliding in the observation area. However, after the cumulative sliding distance exceeded 25 mm, the electric contact began to gradually deteriorate. Finally, after a 50 mm slide, almost no electric current was observed. The electric contact did not recover even when the observation area was changed after the 50 mm slide.

In test #2, using the probe type B, some electric current was measured at the first scan of the tests, but the electric contact was not as stable as that observed in test #1. As the sliding distance increased, the electric contact gradually deteriorated, as in the case of test #1. However, the electric current recovered just after the observation area was changed, as shown in Fig. 2 (b).

In test #3, good electric contact was maintained from the first scan to the last scan after a 50 mm cumulative slide. This result was clearly different from that of test #2, although the only difference between tests #2 and #3 was the substrate material. We performed all the tests twice and found out that they showed good reproducibility.

The FE-SEM images of the probe tip used in tests #1 and #3 are shown in Fig. 2 (c). The Au electrode of probe type A used in test #1 initially protruded, but was significantly worn, whereas the wear was very small at the other contact point on the Si support. On the other hand, the wear of the Si support and the adhesion of the wear debris were observed at the edge of the probe tip used in test #3. This result implies that the Si support and the electrode actually slid simultaneously on the substrate, and they were worn at the same rate as expected.

## 4 Discussion

### 4.1 Modeling of the phenomena

From our previous study [5], we found that the contact pressure between an electrode and a substrate must be several GPa in order to maintain good electric contact. To understand the phenomena that occurred during the tests from the viewpoint of the contact pressure, we assume the model shown in Fig. 3 (a).

Because the surfaces of the Si support and the electrode are always in the same plane, the strain  $\varepsilon$  of these two parts caused by the probe contact force  $N$  must be the same. Therefore, according to Hook's law, the following equation must be satisfied:

$$\varepsilon = p_{Si}/E_{Si} = p_{el}/E_{el} \quad (1)$$

where the Young's modulus and the apparent contact pressures of the Si support and the electrode are  $E_{Si}$ ,  $E_{el}$ ,  $p_{Si}$ , and  $p_{el}$ , respectively. The balance between the probe contact force  $N$  and the apparent contact pressures is

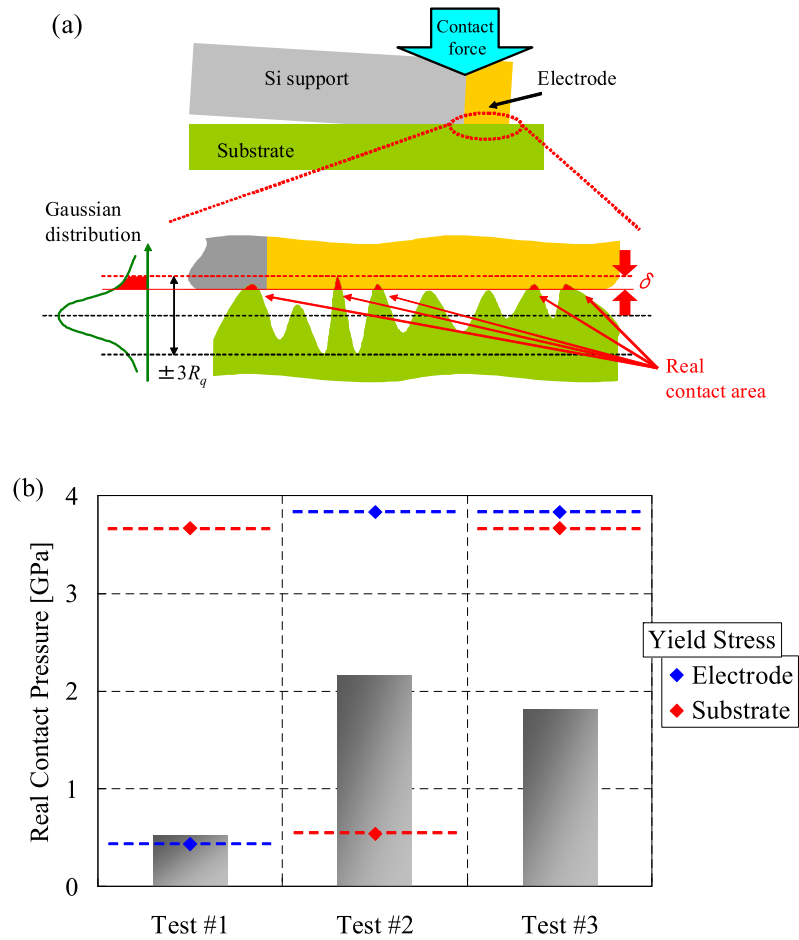


**Fig. 3.** Explanation of the phenomena: (a) diagram of the contact model, (b) results of the contact pressure calculation

expressed as follows:

$$N = A_{Si}p_{Si} + A_{el}p_{el} \quad (2)$$

where the apparent contact areas of the two parts are  $A_{Si}$  and  $A_{el}$ , respectively. Actually, the real contact area is much smaller than its apparent contact area because of the influence of its surface roughness. We define the ratio  $k$  of these two areas as follows:

$$A_{real} = k \cdot A_{apparent} \quad (3)$$

From Eqs. (1), (2), and (3), the real contact pressure of the electrode  $P_{el}$  is expressed as follows:

$$P_{el} = \frac{p_{el}}{k} = \frac{N \cdot E_{el}}{k \cdot (E_{Si}A_{Si} + E_{el}A_{el})}. \quad (4)$$

We consider that the surface roughness of the Si support and the electrode treated by the semiconductor fabrication processes are negligible compared to the roughness of the mechanically polished substrate surface. Also, we assume that 1) the height dispersion of the substrate surface follows a Gaussian distribution, 2) the height of the uppermost part of the substrate surface is

$3R_q$  where  $R_q$  is the root-mean-squared surface roughness because statistically 99.74% of the surface exists within the range of  $\pm 3R_q$ , and 3) the substrate surface contributed to the contact with the electrode distributed within the height range from  $3R_q - \delta$  to  $3R_q$ . Then the ratio  $k$  can be described as follows:

$$k = \frac{1}{2} \left[ 1 - \operatorname{erf} \left( \frac{3R_q - \delta}{\sqrt{2}R_q} \right) \right]. \quad (5)$$

On the other hand, according to the heuristics by Tabor [6], the yield stress of the material can be roughly estimated by the following relation:

$$H \approx 3 \cdot \sigma_{\text{yield}} \quad (6)$$

where  $H$  is the hardness of the material and  $\sigma_{\text{yield}}$  is the yield stress.

From Eqs. (4), (5), and (6), we calculated the values of the real contact pressures and compared them with the yield stresses of the materials. The values of the apparent contact areas  $A_{Si}$  and  $A_{el}$  were estimated from the FE-SEM images of the probe tips used in the tests. The distance  $\delta$  is assumed to be the lattice constant of the substrate materials (Pt: 0.39 nm, Ru: 0.27 nm). The results are shown in Fig. 3 (b). From the viewpoint of the comparison between the contact pressure and the yield stress, the phenomena that occurred during the tests can be explained as follows:

At the beginning of test #1, the sliding system showed very good electric contact because the Au electrode of probe type A initially protruded from the surface of the Si support. However, because Au is much softer than the Ru substrate, the contact area of the electrode increased on account of the wear until the contact pressure became close to the yield stress of Au, which was insufficient to maintain a good electric contact. Therefore, the electric contact was lost and did not recovered even after the observation area was changed.

In test #2, the W probe electrode initially made contact with the Pt substrate with a real contact pressure of more than 2 GPa: hence the sliding system showed good electric contact. However, since the pressure was larger than the yield stress of the Pt substrates, the protrusions on the substrate were rapidly worn and the surface roughness of the substrate decreased. Then the real contact pressure probably decreased to the level of the yield stress of the Pt substrate, and this induced the loss of electric current. This hypothesis is supported by the fact that the electric current recovered when the observation area was changed because the fresh substrate surface with the initial surface roughness regained the real contact pressure for several GPa.

In test #3 only, the yield stresses of both the probe electrode and the substrate were larger than the real contact pressure, although the pressure was nearly 2 GPa, which was enough to establish a good electric contact. Therefore, good electric contact was maintained during the slide without resulting in the rapid wearing of the both surfaces.



## 4.2 Practical implementation

According to the model discussed in the previous section, there are three key factors for maintaining the performance of the anti-wear probes: 1) the probe electrode and the substrate must both be sufficiently hard to maintain a certain level of contact pressure without rapid wearing of the either surface. The support material would have to be just as hard to ensure the stability of the entire sliding system. 2) Flat surfaces are preferable for each part because rough surfaces may initially lead to an increase in the real contact pressure, but protrusions on the surface will easily wear, leading to a reduction of the pressure. 3) Control of the probe contact force is important to keep the contact pressure at the appropriate value.

The LAO lithography that we performed [4] is one of the most suitable applications for the anti-wear probe because both the probe support and the substrate are flat Si wafers. In this case, it is preferable to choose an electrode material which is as hard as Si. W is considered to be one of the good candidates.

On the other hand, our anti-wear probe is not suitable for probe-based data storage systems that use soft polymer films as recording media [2], but it is possible to introduce the anti-wear probe to the storage system using rigid recording media, e.g., ferroelectric materials [3]. To satisfy the aforementioned restrictions, one solution is the deposition of extra bit-patterned top electrodes on the recording substrate. Because then we can control the status of the surface independently from the recording material.

## 5 Conclusion

Evaluation tests of the fabricated anti-wear probes with various electrode materials were performed using the contact mode of an AFM system, and their electric contact stabilities during the slide were measured. The physical contact situation and the wear of the probe tips were observed using FE-SEM.

It was determined that optimal management of the material hardness, surface roughness, and probe contact force was important to enable the probe to exhibit the best performance. Using W as the probe electrode, Si as the probe support, and Ru as the substrate, the aforementioned condition concerning hardness was satisfied, and good electric contact was successfully maintained for a slide of more than 50 mm.

## Acknowledgments

The authors would like to thank the members of the Toshiba Corporate Research and Development Center and Professor M. Sugiyama at the University of Tokyo, for their helpful suggestions. This work was partly supported by the New Energy and Industrial Technology Development Organization (NEDO).